ACS APPLIED MATERIALS & INTERFACES

Research Article

www.acsami.org

Development and Testing of Diglycolamide Functionalized Mesoporous Silica for Sorption of Trivalent Actinides and Lanthanides

Jennifer A. Shusterman,*[,†] Harris E. Mason,[‡] Jon Bowers,[†] Anthony Bruchet,[†] Eva C. Uribe,[†] Annie B. Kersting,[‡] and Heino Nitsche[†,§]

[†]Department of Chemistry, University of California—Berkeley, Berkeley, California 94720, United States

[‡]Glenn T. Seaborg Institute, Physical and Life Sciences Directorate, Lawrence Livermore National Laboratory, L-231, PO Box 808, Livermore, California 94550, United States

Supporting Information

ABSTRACT: Sequestration of trivalent actinides and lanthanides present in used nuclear fuel and legacy wastes is necessary for appropriate long-term stewardship of these metals, particularly to prevent their release into the environment. Organically modified mesoporous silica is an efficient material for recovery and potential subsequent separation of actinides and lanthanides because of its high surface area, tunable ligand selection, and chemically robust substrate. We have synthesized the first novel hybrid material composed of SBA-15 type mesoporous silica functionalized with diglycolamide ligands (DGA-SBA). Because of the high surface area substrate, the DGA-SBA was found to have the highest Eu capacity reported so far in the literature of all DGA solid-phase extractants. The sorption behavior of europium and americium on DGA-SBA in nitric and hydrochloric acid media was tested in batch contact experiments. DGA-SBA was found to have high sorption of Am and Eu in pH 1, 1 M, and 3 M nitric and hydrochloric acid concentrations, which makes it promising for sequestration of these metals from used nuclear fuel or legacy waste. The kinetics of Eu sorption were found to be two times slower than that for Am in 1 M HNO_3. Additionally, the short-term susceptibility of DGA-SBA to degradation in the presence of acid was probed using ^{29}Si and ^{13}C solid-state NMR spectroscopy. The material was found to be relatively stable under these conditions, with the ligand remaining intact after 24 h of contact with 1 M HNO_3, an important consideration in use of the DGA-SBA as an extractant from acidic media.

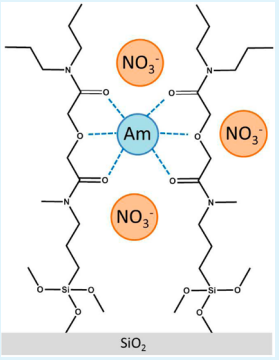

KEYWORDS: *europium, americium, separations, mesoporous silica, diglycolamide, solid-state NMR*

INTRODUCTION

Used nuclear fuel and legacy defense wastes contain significant quantities of trivalent lanthanides and actinides; approximately 10.7 kg of trivalent lanthanides and actinides are present in each ton of used nuclear fuel from pressurized water reactor with typical burnup.[1] The two methods of disposal that are currently being proposed for this waste are either long-term geologic disposal, or partitioning and transmutation of the trivalent actinides.[1] In either disposal regime, separation of the trivalent minor actinides from the fission product lanthanides and from one another could reduce the volume of waste requiring long-term disposal and reduce costs. The trivalent actinides of interest are curium (Cm) and americium (Am). Americium is of special interest as it exists in larger quantities and has a longer half-life than Cm ($t_{1/2}$ (^{241}Am) = 432.6 y vs $t_{1/2}$(^{244}Cm) = 18.1 y). Additionally, the dominant ^{241}Am isotope decays to the long-lived ^{237}Np ($t_{1/2} = 2.144 \times 10^6$ y) and the separation, sequestration, and transmutation of Am has the potential to reduce the lifetime of a geologic nuclear waste repository. The early lanthanides exist as both stable and short-lived fission products in much greater quantities than the aforementioned actinides (>15× more lanthanides than trivalent minor actinides),[1] which complicate separation of the trivalent actinides.[1] Given these challenges, new methods must be developed to facilitate these separations.

The minor actinides and the lanthanides exhibit very similar chemistry in acidic media due to their trivalent charge state and nearly identical ionic radii.[2] As a result, separations based on size exclusion or differences in oxidation state are not frequently successful. Because of the electronic structure of the actinides relative to the lanthanides, their bonds are typically found to be more covalent in nature, allowing for separations that exploit these small differences.[3] Replacing the current liquid–liquid extraction methods[4] with a system based on a solid-phase extractant (SPE) could eliminate the large volumes of hazardous waste generated during separations. A SPE regime would reduce waste volume because of its lack of an organic phase, and there is the potential for reusability.

Solid-phase extractants, or extraction chromatography resins, have been synthesized in many different forms and have been

Received: May 22, 2015
Accepted: September 3, 2015
Published: September 3, 2015

DOI: 10.1021/acsami.5b04481
ACS Appl. Mater. Interfaces 2015, 7, 20591−20599

made commercially available for the purpose of actinide and lanthanide separations. An extraction chromatography resin can be produced by coating, impregnation, or covalent bonding of an extractant ligand to a solid support. The method of production greatly impacts the stability of the overall material. Ligand coating is the most common and easiest synthetic route, and allows the use of a wide variety of ligands since no reactive groups on the inert support structure are necessary. The coated particles, however, often demonstrate poor stability in tests ranging from 1 h to 10 month contact because high acid concentration or radiation dose can cause the ligands to degrade and to fall off the support structure.[5−7] Additionally, large volumes of solution flushing through the solid-phase or the use of high pressure can reduce the lifetime of the coated SPE materials. Impregnating the ligand traps the ligand in either the solid support matrix itself or in a polymer filling of a porous substrate. This procedure is typically done with silica substrates and has the advantage that the ligand is immobilized in the solid support, making it less susceptible to degradation.[8−10] The directionality of the ligand, however, is not easily controlled, resulting in a random ordering of ligands on the surface, which may lower the percentage of available ligands for binding with the metal. Due to the limitations of the first two methods, the present work investigates grafting the ligand with a covalent bond to a solid-support in an effort to add stability and control ligand directionality for improved resins.[11]

The solid-support utilized in this work is SBA-15 type mesoporous (mesoporous defined by 2−50 nm pore diameter) silica. SBA-15 has a well ordered, 2d hexagonal pore structure, with a very high surface area (typically >800 m^2 g^{-1}).[12] Organically modified mesoporous silica has been previously synthesized and utilized for lanthanide and actinide sorption utilizing a variety of ligands.[11,13−19] Diglycolamic acid modified silica substrate have also been studied for lanthanide and actinide uptake.[20,21] The ligand selected for this work is a diglycolamide (DGA). DGA ligands have a similar binding site to the neutral diamide extractants that have been shown to bind trivalent lanthanides and actinides effectively from highly acidic matrices, especially when preorganized.[22,23] Similar to diamides, DGA ligands are composed of only carbon, hydrogen, oxygen, and nitrogen (CHON); therefore, they are completely incinerable at end of use. DGA ligands have been shown to efficiently extract trivalent actinides and lanthanides from highly acidic (>1 M) nitric acidic feeds in the nuclear fuel cycle using solvent extraction.[24−28] DGA has been found to form aggregates in high concentrations of nitric acid that have a high affinity for the trivalent lanthanides and actinides.[29,30] As Chavan et al. discuss,[31] due to this aggregation, preorganization of the DGA on a solid support would should result in a more efficient extraction of Am(III) and Eu(III) than can be achieved with a liquid−liquid system. In the case of diglycolamide-modified mesoporous silica, preorganization of the ligands is done through ligand polymerization during functionalization. Formation of DGA aggregates after contact with nitric acid, as discussed in liquid−liquid systems,[31,32] is not expected because of the covalent bond between the ligand and the silica surface. DGA has been made into a resin by coating it on polymer supports, and is now commercially available.[7,33−36] Some work has been done immobilizing DGA on solid supports via impregnation.[37−39] Recently, Ansari and Mohapatra et al. covalently bound DGA ligands to silica supports for actinide and lanthanide sorption.[40,41] Those materials were found to have lower K_d and capacities values for Eu(III) compared to the SPEs with coated DGA,[34,36] and the authors attribute this to their low ligand loading compared to the other materials.[40,41] Additionally, their materials have multiple amide linkages that can be susceptible to protonation and subsequent hydrolysis. In our current work, we use a different variant of the DGA ligand as well as a different anchor both of which minimize sites that can be protonated. We aim to take advantage of the stability of these grafted solid-phase extractants, but improve upon them by utilizing high surface area mesoporous silica and covalently binding the DGA ligands to the surface to achieve higher ligand loading and in turn greater extraction efficiency.

EXPERIMENTAL SECTION

Material Preparation. Spherical particle SBA-15 type mesoporous silica with 8 nm pore diameter was synthesized based on the procedure from Katiyar et al.[42] The "DGA" ligand was a 4:1 mixture of *N,N*-(dipropyl)-*N*′(methyl), *N*′(3-[trimethoxysilyl]propyl)-3-oxapentane diamide and *N,N*-(dipropyl)-*N*′(methyl), *N*′(3-[monoethoxydimethoxysilyl] propyl)-3-oxapentane diamide (Technocomm, Ltd.) (Figure 1). The DGA ligand was grafted to the silica surface using a solution polymerization technique.[43,44] Condensation of the oxysilanes to the silica surface was conducted under toluene reflux, and then followed by distillation of methanol, water, and a portion of the toluene for volume reduction. The mixture was filtered, washed with 2-propanol, and air-dried overnight. Particles were stored in an evacuated desiccator to prevent exposure to moisture. Detailed synthetic methods are presented in the Supporting Information (SI).

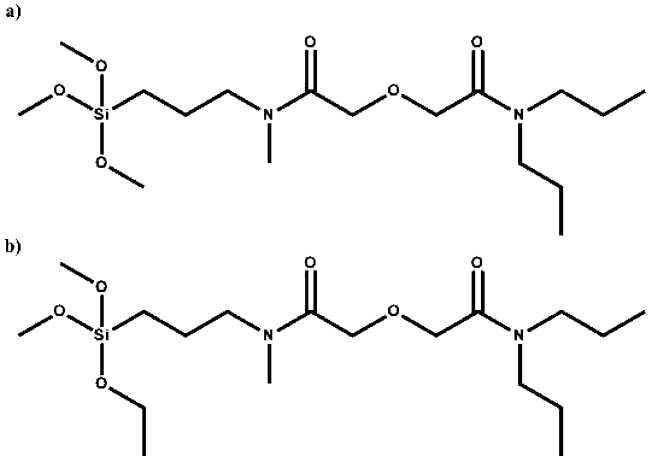

Figure 1. (a) *N,N*-(dipropyl)-*N*′(methyl), *N*′(3-[trimethoxysilyl]-propyl)-3-oxapentane diamide and (b) *N,N*-(dipropyl)-*N*′(methyl), *N*′(3-[monoethoxydimethoxysilyl] propyl)-3-oxapentane diamide. The "DGA" mixture used in the synthesis was a 4 to 1 ratio of a to b.

Characterization. The mesoporous silica was characterized using scanning electron microscopy (SEM), nitrogen adsorption isotherms (BET/BJH method), and IR spectroscopy. The DGA functionalized mesoporous silica (DGA−SBA) was characterized using infrared spectroscopy, thermogravimetric analysis (TGA), nitrogen adsorption isotherms (BET/BJH method), and nuclear magnetic resonance (NMR) spectroscopy. All parameters and methods associated with these techniques are presented in the SI.

Batch Sorption Experiments. Eu(III) stocks were prepared in either pH 3 nitric or hydrochloric acids with a ^{152}Eu tracer. ^{243}Am(III) stock was prepared by purifying the Am(III) (see SI), boiling it to dryness, and redissolving it in either pH 3 nitric or hydrochloric acid. Solid to liquid ratios for all batch experiments were 1 mg solid to 1 mL solution. DGA−SBA solid was pre-equilibrated with the appropriate acid solution (nitric or hydrochloric acid) for 14−17 h after pH adjustment. The pH of the samples in the pH 1−4 range was lowered or raised with the addition of either the acid of interest (HNO_3 or

DOI: 10.1021/acsami.5b04481
ACS Appl. Mater. Interfaces 2015, 7, 20591−20599

HCl) or sodium hydroxide, respectively. The pH of the 1 and 3 M HNO_3 and HCl samples was not measured and the acid concentration of these samples was stoichiometric. Pre-equilibrated samples were spiked with either Eu(III) or Am(III) stock such that the total metal Eu(III) or Am(III) concentration was approximately 10 μM. Solution pH was monitored and adjusted throughout each experiment. Samples were centrifuged at 5000 rpm for 5 min prior to each aliquot removal. Aliquots were removed from the supernatant of the samples at approximately 1, 3, and 24 h after metal addition for the sorption capacity and pH dependence experiments. For the kinetic experiments, aliquots were removed at several time points ranging between 8 min and 9 h after metal addition. To determine Eu sorption capacity, 5 stock solutions of varying Eu concentrations were prepared, such that a 50 μL addition of the appropriate stock to 6 mL 1 M nitric acid would results in Eu concentrations of 75, 125, 250, 500, and 1000 μM.

Desorption experiments were conducted by first contacting preconditioned DGA–SBA with 10 μM Eu or Am in 1 M HNO_3 for 24 h. The samples were centrifuged, and aliquots were taken from the supernatant prior to removal from the solids. Two methods of desorption were tested: (1) rinsing with pH 5 HCl and (2) rinsing with ethylenediaminetetraacetic acid (EDTA). For these two methods, the Eu- or Am-contacted DGA–SBA was rinsed multiple times with 1.5 mL of pH 5.5 HCl or 1 mM EDTA, respectively, taking aliquots of each rinse to monitor desorption. During pre-equilibration and between aliquot removal, samples were rocked top-to-bottom.

The concentration of Eu(III) in the aliquots was monitored via the ^{152}Eu tracer using a high-purity germanium (HPGe) gamma spectrometer quantifying based on the 344 keV gamma peak. Am(III) concentration in the aliquots was measured using liquid scintillation counting (LSC) with Ecolume scintillation cocktail. Percent sorption was calculated relative to the total amount of metal loaded onto the sample (Equation S2). All experiments were conducted in duplicate such that results agreed within 6%. To verify that no precipitation or sorption to the tube was occurring, controls were run in an identical fashion to the samples in the batch sorption experiments, however, they did not contain solid (no-solid blanks). Additional controls with bare SBA-15 were also run in the same manner as the DGA–SBA batch sorption experiments. These were conducted to measure sorption to the bare silica surface with no ligand present. In both the no-solid blanks and the bare SBA-15 controls, no Am(III) or Eu(III) sorption was observed within uncertainty of the measurement under any conditions examined in this work. Error bars represent 1σ and are based on propagation of pipetting, weighing, and counting errors.

RESULTS AND DISCUSSION

Material Characterization. The SEM micrograph of the silica particles indicates that their average shape is spherical (Figure S1). The nitrogen adsorption analysis (Figure S2) of the SBA-15 mesoporous silica measures a surface area of 830 $m^2\ g^{-1}$ and an average pore diameter of 7.5 nm. After functionalization, the surface area and pore diameter decrease to 397 $m^2\ g^{-1}$ and 5.5 nm, respectively. On the basis of the mass loss measured with TGA, the ligand loading per gram of the DGA–SBA was 848 ± 7 μmol g^{-1}. Ligand loading was calculated using a weighted average of the molecular weights of the trimethoxy- and dimethoxymonoethoxysilane attachments on the DGA ligand accounting for the loss of a methoxy- group during grafting (Figure S3, eq (S1)). All of the IR spectra contain the characteristic absorption bands for silica at 1070, 965, 805 cm^{-1} corresponding to the symmetric Si—O—Si stretch, the Si—O stretch of surface silanols, and the antisymmetric Si—O—Si stretch, respectively. In comparing the pristine (as-functionalized) diglycolamide-modified silica, DGA–SBA, (Figure S4b) to the nonfunctionalized SBA (Figure S4a), there is a stretch at 1640 cm^{-1} due to the amide carbonyl stretches of the DGA ligand.

The ^{29}Si{^{1}H} cross-polarization magic angle spinning (CP/MAS) NMR spectrum (Figure 2a) of the pristine solid

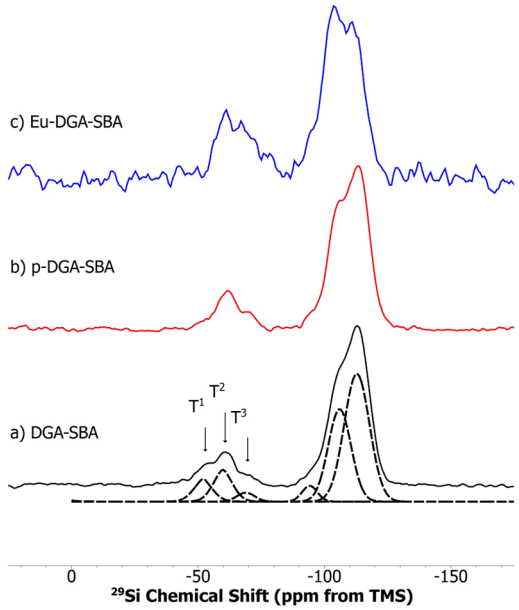

Figure 2. ^{29}Si{^{1}H} CP/MAS NMR spectra for DGA functionalized SBA-15 (a) pristine solid (DGA-SBA), (b) acid-contacted solid (p-DGA–SBA), and (c) Eu-contacted solid (Eu–DGA–SBA) The resonances for the bulk silicon atoms are the Q peaks (Q^2, Q^3, and Q^4 have shifts of δ_{Si} = −94, −104, and −112 ppm, respectively) and for the surface silicon atoms are the T peaks (T^1, T^2, and T^3 have shifts of δ_{Si} = −54, −60, and −69 ppm, respectively). Fits of DGA–SBA with pseudo-Voigt functions indicated with dashed lines directly below the DGA–SBA data.

contained six resonances (Table S1); three are associated with the bulk silica material (Q species, δ_{Si} = −92 to −112 ppm) and three with silicon atoms bound to ligands on the surface (T species, δ_{Si} = −50 to −70 ppm). The Q^n species are defined as $Si(OSi)_n(OH)_{4-n}$ and the T^m species are similarly defined as $SiR(OSi)_m(OH)_{3-m}$.[45,46] Q^4 peaks are from Si atoms bound to four —OSi groups, indicating that they are in the bulk lattice of the silica. Q^3 and Q^2 peaks are both from surface silicon atoms, bound to either 1 or 2 hydroxyl groups, respectively. For bare, nonfunctionalized silica, the ^{29}Si{^{1}H} CP/MAS spectrum only contains Q peaks, so the presence of T peaks indicates that the ligand was covalently bound to the silica surface. T^1 (δ_{Si} = −51 ppm) peaks are a result of ligand monomers on the surface. T^2 (δ_{Si} = −58 ppm) peaks are from Si atoms bound to terminal ligands in a polymer chain, whereas T^3 (δ_{Si} = −69 ppm) peaks are from the Si atoms bound to central ligands in the polymer chain.[45,47] From this spectrum, it is clear that all three species are present. Ideally, the material would be primarily composed of T^2 and T^3 species, indicating polymerization of the ligands. Ligand polymerization is important for complexation with the DGA ligand, as 2–3 ligands are necessary to complex Ln(III) and An(III) of interest depending on the specific metal.[26,48] In addition, ^{13}C{^{1}H} CP/MAS NMR spectrum was used to determine whether the ligand remained intact during the functionalization process. The spectrum shown in Figure 3a contains six resonances (Table S2), three of which were used as evidence that the ligand did not decompose during functionalization: δ_C = 167 ppm (C═O), δ_C= 67 ppm (C—O), and δ_C= 6.7 ppm (—CH_3).[49]

DOI: 10.1021/acsami.5b04481
ACS Appl. Mater. Interfaces 2015, 7, 20591–20599

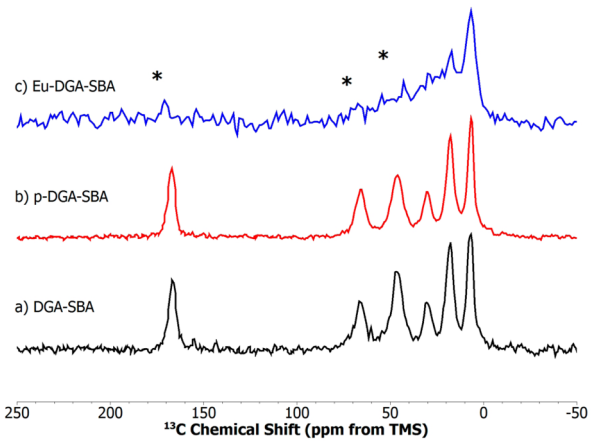

Figure 3. $^{13}C\{^{1}H\}$ CP/MAS NMR spectra for DGA functionalized SBA-15 (a) pristine solid (DGA−SBA), (b) acid-contacted solid (p-DGA−SBA), and (c) Eu-contacted solid (Eu−DGA−SBA). Asterisks indicate chemical shift of resonances impacted by the presence of Eu.

Material Stability in HNO_3. To determine whether the DGA−SBA material would withstand contact with nitric acid for lanthanide and actinide extractions on a lab-scale, the short-term stability of the DGA-SBA in nitric acid was probed. DGA−SBA was contacted with 1 M HNO_3 for 1 day to simulate the conditions used for batch sorption experiments. A $^{29}Si\{^{1}H\}$ CP/MAS NMR spectrum of the acid-contacted sample (Figure 2b) was collected and compared to the pristine material. While CP is inherently not quantitative, peak ratios of the T peaks can still be compared since the spectra were collected under identical conditions.[50] The T peaks were fitted with pseudo-Voigt functions, and the ratios of their integrated peak intensities were calculated. The T^1/T^2 ratios decreased from 0.55 to 0.19 for the pristine compared to the acid degraded sample, respectively. The T^3/T^2 ratios for the pristine and acid degraded sample were 0.27 and 0.29, respectively. The proton spin−lattice relaxation time constants ($T_{1\rho,H}$) for the pristine material were compared to those of the acid-contacted sample because increased protons from the acid can alter the $T_{1\rho,H}$, and in turn, the relative peak intensities. As expected for organically modified silica, the $T_{1\rho,H}$ values for the pristine and acid-contacted samples were similar, averaging 3.1 and 3.2 ms, respectively, which are the same within experimental error (Figure S5). As the $T_{1\rho,H}$ values were the same, the changes in T^1/T^2 ratios is due solely to cleavage of the ligand from the silica surface. The significant decrease observed in T^1/T^2 ratios and relative stability in T^3/T^2 ratios between pristine and acid-contacted samples indicate that the T^2 and T^3 species are not as highly affected by acid contact as T^1 species. The T^1 species substantially hydrolyzed from the surface. The stability of the T^2 and T^3 species relative to the T^1 species indicates that ligand polymerization may potentially help stabilize the functionalized materials to acid-catalyzed hydrolysis.

The $^{13}C\{^{1}H\}$ CP/MAS NMR spectrum of the acid-contacted sample (Figure 3b) shows no substantial difference from the $^{13}C\{^{1}H\}$ CP/MAS NMR spectrum of the pristine sample, indicating that after 1 day of contact with 1 M HNO_3, the ligand does not decompose. While the $^{29}Si\{^{1}H\}$ CP/MAS NMR spectra indicate cleavage of the isolated ligands on the surface, the polymerized ligands remain grafted, and based on the $^{13}C\{^{1}H\}$ CP/MAS NMR spectra, it is clear that the ligands remain intact. The IR spectra of the pristine DGA−SBA (Figure S4b) and the acid-contacted DGA−SBA (Figure S4c) are nearly identical, which agrees with the results from the NMR spectroscopy indicating that the ligand remains intact after short-term acid-contact.

Batch Sorption Experiments. *Eu and Am Kinetics.* The kinetics of Eu and Am sorption to DGA-SBA in 1 M HNO_3 were examined in batch sorption style experiments (Figure 4).

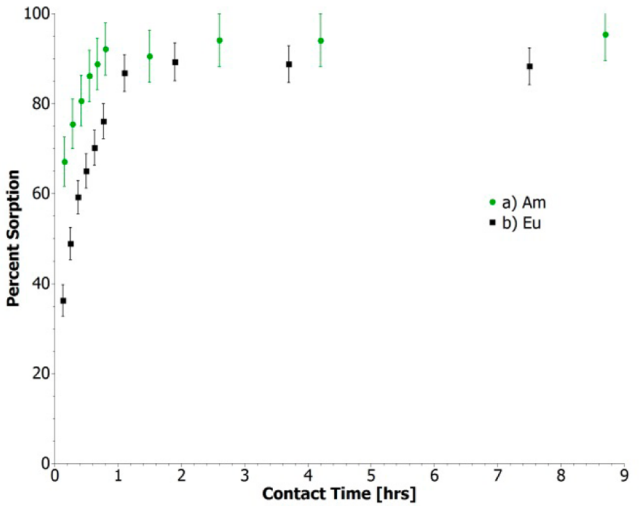

Figure 4. Batch sorption kinetics for (a) Am(III) and (b) Eu(III) from 1 M nitric acid by DGA−SBA. Eu(III) and Am(III) concentrations were 10 and 8 μM, respectively.

The results indicate that Am (Figure 4a) reaches equilibrium after approximately 42 min, whereas Eu (Figure 4b) does not reach equilibrium until it has contacted with the solid for approximately 2 h. The Am and Eu data fit to a pseudo-second-order rate model (Figure S6) with rate constants presented in Table S3. Two parameters that can heavily dictate the sorption kinetics with solid-phase extraction materials are the rates of diffusion through porous substrates and the thermodynamics of the metal−ligand complexation. The observed kinetic behavior is slow for a solid-phase extractant, and this may be the result of the use of a porous substrate and the diffusion time through these pores.[39] However, slow uptake kinetics have also been observed for diglycolamides coated on nonporous silica, which may point to the rate limiting step being the metal−ligand complexation. While, TODGA reaches equilibrium with Am and Eu in just minutes in solvent extraction systems, the immobilization of the ligand may sufficiently change the complexation mechanism resulting in slower kinetics.[51] The difference in sorption kinetics for Eu and Am is likely not because of differences in diffusion as they are similar in size and charge, but may be a result of the relative thermodynamic properties of the Eu−DGA and Am−DGA complexes. The Ln(III)−DGA and An(III)−DGA complexes have been found to have different stability constants in liquid−liquid systems and this should carry over to the solid−liquid system.[52]

Eu and Am Sorption in HNO_3 and HCl. The equilibrium sorption of Eu(III) and Am(III) by DGA−SBA was studied as a function of nitric and hydrochloric acid concentration. As DGA−SBA is mesoporous, it is important to think about the local environment within the pores and how they compare to the bulk sample. Briman et al., discuss the changes in the abundance of pore water as a function of pore surface composition and size, and observed that both of these factors

DOI: 10.1021/acsami.5b04481
ACS Appl. Mater. Interfaces 2015, 7, 20591−20599

contribute to changes in the number of water molecules, but size to a lesser degree.[53] In turn, that may mean that the pH within the pores of the material is not exactly the same as in the bulk sample or compared to other functionalized materials, however, as we are comparing the same material at different acid concentrations, the relative differences should be the same from sample to sample. The concentration of nitric and hydrochloric acid was controlled by molarity for the 3 and 1 M samples and by pH adjustments for the pH 1−4 samples. Results of these experiments after ∼3 h of reaction time are presented in Figure 5. Complete sorption of Eu and Am by

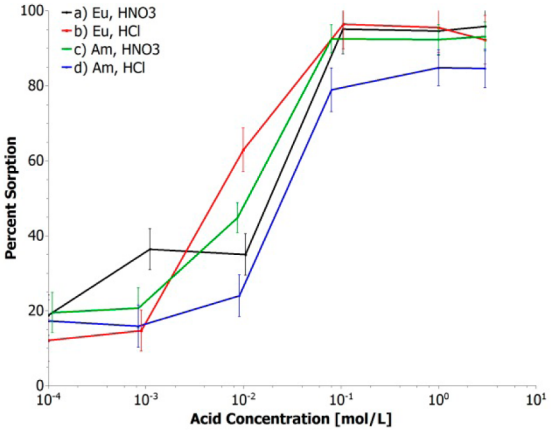

Figure 5. Batch sorption of (a, b) Eu(III) and (c, d) Am(III) from varying concentrations of nitric and hydrochloric acids by DGA−SBA. Metal−solid contact time was approximately 3 h. Eu(III) and Am(III) concentrations were 10 and 8 μM, respectively.

DGA-SBA was observed in pH 1, 1 M, and 3 M HNO_3 solutions. As discussed previously, equilibrium is reached in less than 3 h under the conditions where full sorption occurs, so the sorption data at this time point compared to the 24 h contact data is the same within error. However, at higher pH values, there is not full sorption of either Am or Eu and the samples do not reach equilibrium within 3 h. At the 24 h point, there is substantially decreased sorption in higher pH samples, compared to those at 3 M, 1 M, and pH 1, with 62%, 66%, and 41% sorption at pH 2, 3, and pH 4, respectively. After the same contact time, 78%, 51%, and 45% of the Am sorbs to the DGA-SBA at pH 2, 3, and 4, respectively. While the corresponding K_d values are quite high at all nitric acid concentrations tested, they do vary by 2 orders of magnitude across the acid concentrations tested (Table 1). Those for the highest nitric concentrations (for Eu, 3.2×10^4 and 1.5×10^4 for 1 and 3 M HNO_3, respectively) agree well with the literature for similar materials.[34,36] The substantial increase in sorption as a function of acid concentration is due to the fact that DGA is a neutral extractant and thus binds neutral species. High nitrate or chloride concentrations are required to form the neutral ML_3 complex, where M is Am or Eu and L is Cl^- or NO_3^-. The delay in reaching equilibrium between pH 2 and 4 is because the NO_3^- is more dilute so it takes longer for three of them to come close enough to one another and either Am or Eu to form the neutral complex.

The Eu exhibits similar equilibrium sorption behavior in HCl compared to that in HNO_3. A difference in sorption behavior, however, can be observed at 0.01 M acid concentration where after 24 h of contact, 76% ± 6% of the Eu sorbed in HCl relative to 62% ± 4% in HNO_3 at the same concentration. At

Table 1. Batch Sorption Results of Eu(III) and Am(III) on DGA-SBA after 24 h of Metal Contact Time in HNO_3 and HCl[a]

cation	acid	acid concentration	pH	% sorption	K_d [mL/g]
Eu(III)	HNO_3	3 M		94.1 ± 4.2	1.52×10^4
		1 M		96.3 ± 4.3	3.17×10^4
			0.98	99.8 ± 4.3	2.17×10^5
			1.98	61.9 ± 3.9	1.52×10^3
			2.97	65.6 ± 3.9	1.79×10^3
			3.95	41.2 ± 3.8	6.36×10^2
	HCl	3 M		93.9 ± 6.6	1.41×10^4
		1 M		96.3 ± 6.6	2.45×10^4
			0.98	98.6 ± 6.7	8.12×10^4
			2.00	75.5 ± 6.1	2.84×10^3
			3.04	18.1 ± 5.5	2.13×10^2
			4.01	18.2 ± 5.5	2.10×10^2
Am(III)	HNO_3	3 M		91.8 ± 4.3	1.19×10^4
		1 M		92.8 ± 4.4	1.31×10^4
			1.10	94.6 ± 3.8	1.67×10^4
			2.06	77.9 ± 3.7	3.41×10^3
			3.08	51.4 ± 4.0	1.01×10^3
			3.96	44.7 ± 4.7	7.68×10^2
	HCl	3 M		88.4 ± 5.0	7.33×10^3
		1 M		88.9 ± 4.8	7.74×10^3
			1.10	84.6 ± 4.7	5.39×10^3
			2.04	43.0 ± 5.7	7.37×10^2
			3.08	32.3 ± 5.2	4.64×10^2
			3.99	40.2 ± 5.0	5.92×10^2

[a]Metal ion concentrations were 8 μM and 10 μM for Am(III) and Eu(III), respectively.

0.1, 1, and 3 M HCl, Eu sorption was identical to sorption from HNO_3, which resulted in nearly complete sorption from a 10 μm Eu solution. Interestingly, Am did not have as high sorption in HCl at concentrations of 0.01, 1, and 3 M and higher as Eu. At the very high acid concentrations tested, Am sorption never reaches 95−100%, as observed in HNO_3. After 24 h in 0.01 M HCl, Eu has much higher sorption than Am, 76% ± 6% relative to 43% ± 6%, respectively. This difference could be utilized in chromatographic separations. In terms of K_d values, that correlates to 2.8×10^3 (Eu) and 7.4×10^2 (Am) after 24 h of metal−solid contact time, resulting in a separation factor of Eu to Am of 3.8. Separation factors at equilibrium derived from batch experiments, however, do not always accurately predict the separations that can be achieved in a chromatographic separation as the solid/liquid ratios and kinetics are significantly different in these two cases and column characteristics must be taken into account.[54] By combining the slightly different behavior in hydrochloric acid especially at shorter contact times, a chromatographic separation of Am from Eu may be possible using DGA-SBA as a solid-phase. Future work will include testing the chromatographic potential of DGA-SBA.

Eu Sorption Capacity. The sorption capacity of DGA-SBA was determined for Eu(III) in 1 M HNO_3 (Figure S7). On the basis of the overall similar chemistry of Eu(III) and Am(III) in 1 M HNO_3, we expect that their sorption capacity will be similar under these conditions, and Eu is much less costly than the ^{243}Am required for this measurement. For this experiment, stocks of varying Eu concentrations were added to samples of the same DGA-SBA mass and acid volume and concentration.

DOI: 10.1021/acsami.5b04481
ACS Appl. Mater. Interfaces 2015, 7, 20591−20599

The capacity was determined from the concentration of Eu measured in the supernatant after 24 h of contact. Two different adsorption isotherm models, Langmuir (Figure S8) and Freundlich (Figure S9), were used. A linear regression was applied, and the sorption data were best described with a Langmuir isotherm. From the Langmuir fit, the sorption capacity of the DGA-SBA for Eu(III) was found to be 379 μmol g^{-1}. On the basis of the TGA data and measured capacity, we have calculated the ligand-to-metal ratio. The raw TGA data are mass loss for a preweighed mass of functionalized silica. The moles of ligand volatilized per gram of DGA-SBA are 848 μmol g^{-1}. The sorption capacity determined through the Langmuir isotherm is 379 μmol g^{-1}. Thus, the ratio of ligand to metal comes to an average of 2.2 ligands per metal.

As with any model, however, it is important to keep in mind the assumptions and limitations. The Langmuir model assumes a smooth surface and monolayer sorption. The Freundlich model, however, better accounts for a more heterogeneous surface. On the basis of the surface coverage of the ligand determined by TGA and the presence of T^1 species in the $^{29}Si\{^1H\}$ CP/MAS NMR spectrum, there is not a complete monolayer of ligand on the surface. The better fit of the Langmuir model compared to Freundlich may indicate that the Eu is primarily interacting in areas of local well-ordered monolayer formation.

Eu and Am Desorption. As expected based on previous work,[36,41] EDTA was effective at completely desorbing Am from the DGA-SBA. While one rinse with 1 mM EDTA for 1 h only removed 12% of the Am, a second rinse for the same amount of time desorbed an additional 82% of the original Am, and third rinse successfully removed the remaining Am. The low percent desorption of Am during the first rinse with EDTA is likely the result of minimal EDTA deprotonation ($pK_{a,1}$ = 2.0) due to the low pH caused by remaining 1 M HNO_3 from the sorption process. Similarly, desorption of Eu from the DGA-SBA using 1 mM EDTA was tested. The desorption of Eu with EDTA was not quite as successful as it was for Am, with a maximum of 80% of the Eu being removed after 3 h-long rinses. The first and second rinses desorbed approximately 10% and 75%, respectively. The lower overall desorption of Eu compared to Am may be indicative of a stronger Eu−DGA complex relative to the Am−DGA complex and agrees with the higher K_d observed for Eu compared to Am in 1 M HNO_3 (Table 1). While an hour long desorption may seem to be impractical for a chromatographic application, the column experiment presented later in this work demonstrates faster desorption in EDTA in which 100% of the Eu was stripped from the DGA−SBA. Desorption experiments using dilute HCl were attempted, however, they were less successful than those done with EDTA (see SI).

Complexation in Eu−DGA−SBA. The complexation of Eu to the DGA−SBA was explored using $^{29}Si\{^1H\}$ and $^{13}C\{^1H\}$ CP/MAS NMR experiments (Figures 2c and 3c, respectively). Eu exhibits van Vleck paramagnetism, so in the $^{29}Si\{^1H\}$ and $^{13}C\{^1H\}$ CP/MAS NMR spectra, Si and C nuclei that are near enough to the Eu center will experience the influence of its paramagnetism.[55−58] This result is exhibited with a change in their chemical shift and relaxation behavior. The Eu−DGA−SBA sample was preconditioned with 1 M HNO_3 prior to Eu addition and subsequent sorption for a 24 h time period. The filtered, washed, and dried sample was then studied with NMR spectroscopy. In the $^{13}C\{^1H\}$ CP/MAS NMR spectra of Eu−DGA−SBA compared to p-DGA−SBA (Figure 3, parts c and b, respectively), it is clear that the intensity of the resonances at δ_C = 167, 67, and 47 ppm (marked by asterisks on Figure 3c) have decreased substantially with the addition of Eu. This is not evidence of the ligand decomposing due to acid, as that would have resulted in these peaks also decreasing in the p-DGA−SBA, but rather a result of the paramagnetic nature of the Eu bound to the ligands. The carbon atoms that are directly bound to the oxygen atoms are most affected, as these are the closest to the binding site (carbonyl and ether oxygens). However, even carbon atoms that were more distant from the binding site were impacted by the Eu, indicating that the paramagnetic influence could be extending beyond just a few angstroms. The remaining, most intense resonance at δ_C = 6.7 ppm indicate that the —CH_3 carbons are distant from the Eu.

To verify that the decrease in intensity of the peaks at δ_C = 167, 66, and 47 ppm was not due to Eu-catalyzed ligand breakdown, an IR spectrum of the Eu−DGA−SBA sample was collected. The results of the IR measurement of the Eu−DGA−SBA indicates the carbonyl stretch is still present but shifted to 1620 cm^{-1} (Figure S4d) compared to 1640 cm^{-1} in the acid pretreated solid (Figure S4c). This shift indicates that the ligand is still present and intact, and that the Eu is coordinating through the carbonyls, as expected.[59] Additionally, the intensity of the symmetric Si—O—Si stretch at 1070 cm^{-1} decreased significantly in the Eu−DGA−SBA sample. This decrease may be indicative of a change in the linearity of the bulk silica.[60] One could imagine that prior to complexation, the ligands on the surface can rotate and bend freely. However, with two or more ligands complexing to a single Eu atom, they lose much of their original rotational and bending freedom. Restraining the ligands through complexation could result in overall increased rigidity of the surface layers of the bulk silica.

The ^{13}C NMR spectrum clearly confirms that the Eu is binding directly to the ligand, through the expected tridentate binding site. To determine if the Eu is also interacting strongly with the silica surface, a $^{29}Si\{^1H\}$ CP/MAS NMR spectrum was collected on the Eu−DGA−SBA (Figure 2c). The ^{29}Si NMR spectrum for the Eu−DGA−SBA still contains both T and Q peaks, and the T peak ratios are quite similar to those observed in the p-DGA−SBA. However, the Q^3/Q^4 ratio changed, which could be a result of Eu altering the CP kinetics of these peaks.[61]

Column Study. To verify that DGA-SBA could be used as a stationary phase for a column, a proof-of-principle experiment was done using Eu(III). A Pt-tipped glass column was packed with a DGA-SBA slurry, capping the resin bed on either end with glass wool. The column volume (CV) was approximately 170 μL, with a resin height of 2 cm. The flow rate was about 12 drops per min (120 μL per min). The resin was conditioned with 15 CVs of 1 M HNO_3 prior to loading 75 μL of 1.2 mM Eu(III), which was added as $Eu(NO_3)_3$ with a ^{152}Eu tracer in 1 M HNO_3. The column was washed with 5.5 CVs of 1 M HNO_3 then eluted with 17 CVs of 1 mM EDTA. The resulting elution curve is presented in Figure 6. All of the Eu that was loaded onto the column was eluted in the EDTA fractions, and there was no breakthrough of Eu during the 1 M HNO_3 wash fractions. As evident in the elution curve, there is tailing of the Eu peak which may be a result of the diffusion through the porous structure; however, this requires further investigation.

CONCLUSIONS

Previous studies have immobilized diglycolamide ligands on silica,[36,40,41] but this is the first time these ligands have been covalently bound to mesoporous silica, a much higher surface

DOI: 10.1021/acsami.5b04481
ACS Appl. Mater. Interfaces 2015, 7, 20591−20599

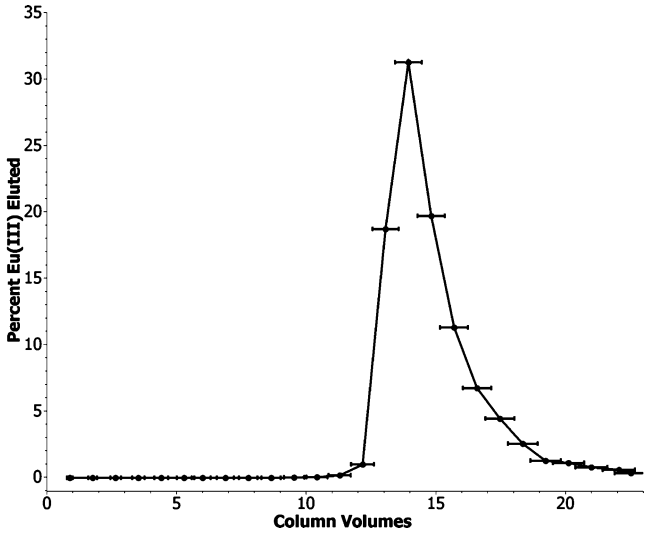

Figure 6. Loading and elution curve for Eu(III) on a column containing DGA−SBA as the stationary phase. Conditioning, loading, and washing were all done with 1 M HNO_3. Eu(III) was eluted in 1 mM EDTA. Vertical error bars represent counting error and are too small to be visible on the scale of this figure.

area substrate. The result of using mesoporous silica is that the material has a higher surface area (397 m^2 g^{-1}) and in turn a higher metal ion capacity compared to an analogous DGA resin that was not on a mesoporous substrate (substrate surface area: 180 m^2 g^{-1}).[36] The advantage to a higher capacity solid-phase extractant is the smaller amount of solid that can be used while still providing the same functional number of ligands to the metal. The Eu(III) sorption capacity determined for the DGA−SBA presented here was 379 μmol g^{-1} (57 mg g^{-1}) which is four times higher than the higher capacity analogous resin (14 mg g^{-1}) presented by Verboom et al.[36] In comparing Eu sorption from 3 M HNO_3 for the DGA-SBA to the same analogous resins, the DGA−SBA has a much higher K_d at 2.4×10^4 relative to 2.7×10^3 and 5.7×10^3 for the two resins made by Verboom et al. The same trend is observed for Am; however, these results are not directly comparable as the metal ion concentrations were significantly higher in this work compared to those in the literature. The higher K_d values are likely due to the higher surface area and in turn, higher ligand loading, of the DGA−SBA material.

The ligand loading for the commercially available DGA resin[34] material is lower at approximately 688 μmol g^{-1}, however, has a higher ligand density of 0.83 silanes per nm^2 (based on 500 m^2 g^{-1} surface area[62] of Amberchrom-CG71) which is likely due to a thicker ligand layer in the coated material than is possible with a covalently bound material. Eu sorption capacity, for the DGA−SBA is again higher compared to the commercially available resin (379 μmol g^{-1} vs 203 μmol g^{-1}). The higher capacity for DGA−SBA despite the lower ligand density supports the hypothesis that the coated solid-phase extractants leave many ligands inaccessible to the metal, whereas covalently bound ligands are more accessible. DGA−SBA has the highest Eu(III) capacity of all diglycolamide solid-phase extractants thus reported.[34,36]

DGA−SBA sorbed Eu and Am effectively in acid concentrations between 0.1 and 3 M. The nearly complete sorption of both Am(III) and Eu(III) from nitric and hydrochloric acid at these concentrations is promising for sequestration of these metals with DGA−SBA from dissolved used nuclear fuel or legacy waste. Additionally, the stability of the ligand in the presence of acid indicates that the DGA−SBA could be used as a solid-phase extractant without substantial degradation during the course of an experiment. EDTA was effective in completely desorbing the metals from the DGA−SBA. While it is not ideal to use an organic complexing agent to desorb, especially when trying to eliminate hazardous organic waste production, the overall volume and concentration of EDTA is low relative to a liquid−liquid extraction. The efficacy of EDTA at desorbing Eu(III) was demonstrated in a column experiment in which Eu(III) was completely eluted from the column using a small volume of EDTA.

Am was found to have faster sorption kinetics relative to Eu that follow a pseudo-second order rate law. Additionally, over twice the amount of Eu sorbed to the DGA-SBA relative to Am in 0.01 M HCl. The difference in sorption behavior for Am and Eu at 0.01 M HCl could potentially be utilized for a separation, especially if coupled with the difference in sorption kinetics, however, this would require detailed further study. If Am and Eu could be separated using DGA-SBA, then it would not only be an efficient bulk sequestration agent for trivalent actinides and lanthanides, but could also potentially be used to isolate Am from the lanthanide fission products.

■ ASSOCIATED CONTENT

Supporting Information

This material is available at The Supporting Information is available free of charge on the ACS Publications website at DOI: 10.1021/acsami.5b04481.

Material synthesis and characterization methods, results from TGA and nitrogen adsorption/desorption isotherms, peak information for NMR spectra, kinetic fitting, SEM micrograph, IR spectra, and sorption capacity and isotherms (PDF)

■ AUTHOR INFORMATION

Corresponding Author

*E-mail: Jennifer.Shusterman@berkeley.edu (J.S.).

Notes

The authors declare no competing financial interest.

[§]Deceased.

■ ACKNOWLEDGMENTS

The authors would like to thank Professors Katz and Long of the University of California—Berkeley for the TGA and nitrogen adsorption measurements, respectively. The authors would also like to thank Professors Long and Yang of the University of California—Berkeley for use of the SEM and IR instruments. The authors would like to thank E. May of the University of California—Berkeley for assistance in counting samples for the column experiments. This work was supported by the National Nuclear Security Administration (NNSA) under the Stewardship Science Academic Alliance Program, award number DE-NA0001978 and by the Subsurface Biogeochemical Research Program of the U.S. Department of Energy's Office of Biological and Environmental Research. This work was performed under the auspices of the U.S. Department of Energy by Lawrence Livermore National Laboratory under Contract DE-AC52-07NA27344. J.S. is supported by a DOE NNSA Stewardship Science Graduate Fellowship under Contract No. DE-NA0002135. E.C.U is supported by a

DOI: 10.1021/acsami.5b04481
ACS Appl. Mater. Interfaces 2015, 7, 20591−20599

National Science Foundation Graduate Research Fellowship under Grant No. DGE 1106400.

REFERENCES

(1) Nuclear Energy Agency. *Physics and Safety of Transmutation Systems*; 2006.

(2) Shannon, R. D. Revised Effective Ionic Radii and Systematic Studies of Interatomic Distances in Halides and Chaleogenides. *Acta Crystallogr., Sect. A: Cryst. Phys., Diffr., Theor. Gen. Crystallogr.* **1976**, *A32*, 751−767.

(3) Jensen, M. P.; Bond, A. H. Comparison of Covalency in the Complexes of Trivalent Actinide and Lanthanide Cations. *J. Am. Chem. Soc.* **2002**, *124*, 9870−9877.

(4) Lewis, F.; Hudson, M.; Harwood, L. Development of Highly Selective Ligands for Separations of Actinides from Lanthanides in the Nuclear Fuel Cycle. *Synlett* **2011**, *2011*, 2609−2632.

(5) Panja, S.; Mohapatra, P. K.; Misra, S. K.; Tripathi, S. C. Carrier Facilitated Transport of Europium(III) Across Supported Liquid Membranes Containing N,N,N ′, N ′-Tetra-2-Ethylhexyl-3-Oxapentane-Diamide (T2EHDGA) as the Extractant. *Sep. Sci. Technol.* **2011**, *46*, 1941−1949.

(6) Klug, C.; Sudowe, R. A Novel Extraction Chromatography Resin for Trivalent Actinides Using 2,6-bis(5,6-Diisobutyl-1,2,4-Triazine-3-Yl)pyridine. *Sep. Sci. Technol.* **2013**, *48*, 2567−2575.

(7) Ansari, S. a; Pathak, P. N.; Husain, M.; Prasad, a K.; Parmar, V. S.; Manchanda, V. K. Extraction Chromatographic Studies of Metal Ions Using N,N,N′,N′-Tetraoctyl Diglycolamide as the Stationary Phase. *Talanta* **2006**, *68*, 1273−1280.

(8) Hoshi, H.; Wei, Y.-Z.; Kumagai, M.; Asakura, T.; Morita, Y. Separation of Trivalent Actinides from Lanthanides by Using R-BTP Resins and Stability of R-BTP Resin. *J. Alloys Compd.* **2006**, *408−412*, 1274−1277.

(9) Liu, R.; Wang, X.; Wei, Y.; Shi, W.; Chai, Z. Evaluation Study on a Macroporous Silica-Based Isohexyl-BTP Adsorbent for Minor Actinides Separation from Nitric Acid Medium. *Radiochim. Acta* **2014**, *102*, 93−100.

(10) Wei, Y.; Kumagai, M.; Takashima, Y.; Modolo, G.; Odoj, R. Studies on the Separation of Minor Actinides from High-Level Wastes by Extraction Chromatography Using Novel Silica-Based Extraction Resins. *Nucl. Technol.* **2000**, *132*, 413−423.

(11) Fryxell, G. E.; Mattigod, S. V.; Lin, Y.; Wu, H.; Fiskum, S.; Parker, K.; Zheng, F.; Yantasee, W.; Zemanian, T. S.; Addleman, R. S.; Liu, J.; Kemner, K.; Kelly, S.; Feng, X. Design and Synthesis of Self-Assembled Monolayers on Mesoporous Supports (SAMMS): The Importance of Ligand Posture in Functional Nanomaterials. *J. Mater. Chem.* **2007**, *17*, 2863−2874.

(12) Zhao, D.; Feng, J.; Huo, Q.; Melosh, N.; Fredrickson, G. H.; Chmelka, B. F.; Stucky, G. D. Triblock Copolymer Syntheses of Mesoporous Silica with Periodic 50 to 300 Angstrom Pores. *Science (Washington, DC, U. S.)* **1998**, *279*, 548−552.

(13) Bourg, S.; Broudic, J.-C.; Conocar, O.; Moreau, J. J. E.; Meyer, D.; Wong Chi Man, M. Tailoring of Organically Modified Silicas for the Solid−Liquid Extraction of Actinides. *Chem. Mater.* **2001**, *13*, 491−499.

(14) Fryxell, G. E.; Lin, Y.; Fiskum, S.; Birnbaum, J. C.; Wu, H.; Kemner, K.; Kelly, S. Actinide Sequestration Using Self-Assembled Monolayers on Mesoporous Supports. *Environ. Sci. Technol.* **2005**, *39*, 1324−1331.

(15) Fryxell, G. E.; Wu, H.; Lin, Y.; Shaw, W. J.; Birnbaum, J. C.; Linehan, J. C.; Nie, Z.; Kemner, K.; Kelly, S. Lanthanide Selective Sorbents: Self-Assembled Monolayers on Mesoporous Supports (SAMMS). *J. Mater. Chem.* **2004**, *14*, 3356−3363.

(16) Zhang, W.; He, X.; Ye, G.; Yi, R.; Chen, J. Americium(III) Capture Using Phosphonic Acid-Functionalized Silicas with Different Mesoporous Morphologies: Adsorption Behavior Study and Mechanism Investigation by EXAFS/XPS. *Environ. Sci. Technol.* **2014**, *48*, 6874−6881.

(17) Fryxell, G. E.; Chouyyok, W.; Rutledge, R. D. Design and Synthesis of Chelating Diamide Sorbents for the Separation of Lanthanides. *Inorg. Chem. Commun.* **2011**, *14*, 971−974.

(18) Trens, P.; Russell, M. L.; Spjuth, L.; Hudson, M. J.; Liljenzin, J.-O. Preparation of Malonamie-MCM-41 Materials for the Heterogeneous Extraction of Radionuclides. *Ind. Eng. Chem. Res.* **2002**, *41*, 5220−5225.

(19) Yuan, L. Y.; Bai, Z. Q.; Zhao, R.; Liu, Y. L.; Li, Z. J.; Chu, S. Q.; Zheng, L. R.; Zhang, J.; Zhao, Y. L.; Chai, Z. F.; Shi, W. Q. Introduction of Bifunctional Groups into Mesoporous Silica for Enhancing Uptake of thorium(IV) from Aqueous Solution. *ACS Appl. Mater. Interfaces* **2014**, *6*, 4786−4796.

(20) Shkrob, I. a.; Tisch, A. R.; Marin, T. W.; Muntean, J. V.; Kaminski, M. D.; Kropf, A. J. Surface Modified, Collapsible Controlled Pore Glass Materials for Sequestration and Immobilization of Trivalent Metal Ions. *Ind. Eng. Chem. Res.* **2011**, *50*, 4686−4696.

(21) Suneesh, A. S.; Syamala, K. V.; Venkatesan, K. A.; Antony, M. P.; Vasudeva Rao, P. R. Diglycolamic Acid Modified Silica Gel for the Separation of Hazardous Trivalent Metal Ions from Aqueous Solution. *J. Colloid Interface Sci.* **2015**, *438*, 55−60.

(22) Lumetta, G.; Rapko, B.; Hay, B.; Garza, P.; Gilbertson, R.; Hutchison, J. A Novel Bicyclic Diamide with High Binding Affinity for Trivalent f-Block Elements. *Solvent Extr. Ion Exch.* **2003**, *21*, 29−39.

(23) Spjuth, L.; Liljenzin, J. O.; Hudson, M. J.; Drew, M. G. B.; Iveson, P. B.; Madic, C. Comparison of Extraction Behaviour and Basicity of Some Substituted Malonamides. *Solvent Extr. Ion Exch.* **2000**, *18*, 1−23.

(24) Sasaki, Y.; Tachimori, S. Extraction of Actinides(III), (IV), (V), (VI), and Lanthanides(III) by Structurally Tailored Diamides. *Solvent Extr. Ion Exch.* **2002**, *20*, 21−34.

(25) Suzuki, B. H.; Sasaki, Y.; Sugo, Y.; Apichaibukol, A.; Kimura, T. Extraction and Separation of Am (III) and Sr (II) by N, N, N, N -Tetraoctyl-3-Oxapentanediamide (TODGA). *Radiochim. Acta* **2004**, *92*, 463−466.

(26) Sasaki, Y.; Sugo, Y.; Suzuki, S.; Tachimori, S. The Novel Extractants, Diglycolamides, for the Extraction of Lanthanides and Actinides in HNO3-N-Dodecane System. *Solvent Extr. Ion Exch.* **2001**, *19*, 91−103.

(27) Kimura, T.; Choppin, G. Luminescence Study on Determination of the Hydration Number of Cm(III). *J. Alloys Compd.* **1994**, *213-214*, 313−317.

(28) Gelis, A. V.; Lumetta, G. J. Actinide Lanthanide Separation Process—ALSEP. *Ind. Eng. Chem. Res.* **2014**, *53*, 1624−1631.

(29) Jensen, M. P.; Yaita, T.; Chiarizia, R. Reverse-Micelle Formation in the Partitioning of Trivalent F-Element Cations by Biphasic Systems Containing a Tetraalkyldiglycolamide. *Langmuir* **2007**, *23*, 4765−4774.

(30) Yaita, T.; Herlinger, a. W.; Thiyagarajan, P.; Jensen, M. P. Influence of Extractant Aggregation on the Extraction of Trivalent F-Element Cations by a Tetraalkyldiglycolamide. *Solvent Extr. Ion Exch.* **2004**, *22*, 553−571.

(31) Chavan, V.; Thekkethil, V.; Pandey, A. K.; Iqbal, M.; Huskens, J.; Singh, S.; Goswami, A.; Verboom, W. Assembled Diglycolamide for F-Element Ions Sequestration at High Acidity. *React. Funct. Polym.* **2014**, *74*, 52−57.

(32) Chavan, V.; Patra, S.; Pandey, A. K.; Thekkethil, V.; Iqbal, M.; Huskens, J.; Sen, D.; Mazumder, S.; Goswami, A.; Verboom, W. Understanding Nitric Acid-Induced Changes in the Arrangement of Monomeric and Polymeric Methacryloyl Diglycolamides on Their Affinity toward F-Element Ions. *J. Phys. Chem. B* **2015**, *119*, 212−218.

(33) Husain, M.; Ansari, S.; Mohapatra, P.; Gupta, R.; Parmar, V.; Manchanda, V. Extraction Chromatography of Lanthanides Using N,N,N′,N′-Tetraoctyl Diglycolamide (TODGA) as the Stationary Phase. *Desalination* **2008**, *229*, 294−301.

(34) Horwitz, E. P.; McAlister, D. R.; Bond, A. H.; Barrans, R. E., Jr. Novel Extraction of Chromatographic Resins Based on Tetraalkyldiglycolamides: Characterization and Potential Applications. *Solvent Extr. Ion Exch.* **2005**, *23*, 319−344.

DOI: 10.1021/acsami.5b04481
ACS Appl. Mater. Interfaces 2015, 7, 20591−20599

(35) Gharibyan, N.; Dailey, A.; McLain, D. R.; Bond, E. M.; Moody, W. a.; Happel, S.; Sudowe, R. Extraction Behavior of Americium and Curium on Selected Extraction Chromatography Resins from Pure Acidic Matrices. *Solvent Extr. Ion Exch.* **2014**, *32*, 391−407.
(36) Ansari, S. A.; Mohapatra, P. K.; Iqbal, M.; Huskens, J.; Verboom, W. Two Novel Extraction Chromatography Resins Containing Multiple Diglycolamide-Functionalized Ligands: Preparation, Characterization and Actinide Uptake Properties. *J. Chromatogr. A* **2014**, *1334*, 79−86.
(37) Modolo, G.; Asp, H.; Schreinemachers, C.; Vijgen, H. Recovery of Actinides and Lanthanides from High-Level Liquid Waste by Extraction Chromatography Using TODGA+TBP Impregnated Resins. *Radiochim. Acta* **2007**, *95*, 391−397.
(38) Zhang, A.; Mei, C.; Wei, Y.; Kumagai, M. Preparation of a Novel Macroporous Silica-Based Diglycolamide Derivative-Impregnated Polymeric Composite and Its Adsorption Mechanism for Rare Earth Metal Ions. *Adsorpt. Sci. Technol.* **2007**, *25*, 257−272.
(39) Van Hecke, K.; Modolo, G. Separation of Actinides from Low Level Liquid Wastes (LLLW) by Extraction Chromatography Using Novel DMDOHEMA and TODGA Impregnated Resins. *J. Radioanal. Nucl. Chem.* **2004**, *261*, 269−275.
(40) Mohapatra, P. K.; Ansari, S. A.; Iqbal, M.; Huskens, J.; Verboom, W. First Example of Diglycolamide-Grafted Resins: Synthesis, Characterization, and Actinide Uptake Studies. *RSC Adv.* **2014**, *4*, 10412−10419.
(41) Ansari, S. A.; Mohapatra, P. K.; Iqbal, M.; Huskens, J.; Verboom, W. Sorption of americium(III) and europium(III) from Nitric Acid Solutions by a Novel Diglycolamide-Grafted Silica-Based Resins: Part 2. Sorption Isotherms, Column and Radiolytic Stability Studies. *Radiochim. Acta* **2014**, *102*, 903−910.
(42) Katiyar, A.; Yadav, S.; Smirniotis, P. G.; Pinto, N. G. Synthesis of Ordered Large Pore SBA-15 Spherical Particles for Adsorption of Biomolecules. *J. Chromatogr. A* **2006**, *1122*, 13−20.
(43) Fryxell, G. E.; Liu, J. Designing Surface Chemistry in Mesoporous Silica. In *Adsorption on Silica Surfaces*; Papirer, E., Ed.; 2000; pp 665−687.
(44) Feng, X.; Fryxell, G. E.; Wang, L.-Q.; Kim, A. Y.; Liu, J.; Kemner, K. M. Functionalized Monolayers on Ordered Mesoporous Supports. *Science (Washington, DC, U. S.)* **1997**, *276*, 923−926.
(45) Bibent, N.; Charpentier, T.; Devautour-Vinot, S.; Mehdi, A.; Gaveau, P.; Henn, F.; Silly, G. Solid-State NMR Spectroscopic Studies of Propylphosphonic Acid Functionalized SBA-15 Mesoporous Silica: Characterization of Hydrogen-Bonding Interactions. *Eur. J. Inorg. Chem.* **2013**, *2013*, 2350−2361.
(46) Bendjeriou-Sedjerari, A.; Pelletier, J. D. A.; Abou-hamad, E.; Emsley, L.; Basset, J.-M. A Well-Defined Mesoporous Amine Silica Surface via a Selective Treatment of SBA-15 with Ammonia. *Chem. Commun.* **2012**, *48*, 3067−3069.
(47) Shusterman, J. A.; Mason, H. E.; Bruchet, A.; Zavarin, M.; Kersting, A. B.; Nitsche, H. Analysis of Trivalent Cation Complexation to Functionalized Mesoporous Silica Using Solid-State NMR Spectroscopy. *Dalt. Trans.* **2014**, *43*, 16649−16658.
(48) Antonio, M. R.; McAlister, D. R.; Horwitz, E. P. An Europium(iii) Diglycolamide Complex: Insights into the Coordination Chemistry of Lanthanides in Solvent Extraction. *Dalton Trans.* **2015**, *44*, 515−521.
(49) Iqbal, M.; Mohapatra, P. K.; Ansari, S. a.; Huskens, J.; Verboom, W. Preorganization of Diglycolamides on the calix[4]arene Platform and Its Effect on the Extraction of Am(III)/Eu(III). *Tetrahedron* **2012**, *68*, 7840−7847.
(50) Sindorf, D. W.; Maciel, G. E. 29Si CP/MAS NMR Studies of Methylchlorosilane Reactions on Silica Gel. *J. Am. Chem. Soc.* **1981**, *103*, 4263−4265.
(51) Sasaki, Y.; Sugo, Y.; Tachimori, S. Actinide Separation with a Novel Tridentate Ligand, Diglycolic Amide for Application to Partitioning Process. In *ATALANTE 2000—Scientific Research on the Back-end of the Fuel Cycle for the 21st Century*; 2000; pp 02−07.
(52) Charbonnel, M.-C.; Berthon, C.; Berthon, L.; Boubals, N.; Burdet, F.; Duchesne, M.-T.; Guilbaud, P.; Mabille, N.; Petit, S.; Zorz, N. Complexation of Ln(III) and Am(III) with the Hydrosoluble TEDGA: Speciation and Thermodynamics Studies. *Procedia Chem.* **2012**, *7*, 20−26.
(53) Briman, I. M.; Re, D.; Diat, O.; Zanotti, J.; Jollivet, P. Impact of Pore Size and Pore Surface Composition on the Dynamics of Confined Water in Highly Ordered Porous Silica. *J. Phys. Chem. C* **2012**, *116*, 7021−7028.
(54) Gharibyan, N. *Intragroup Separation of Trivalent Lanthanides and Actinides for Neutron Capture Experiments in Stockpile Stewardship Sciences*; University of Nevada: Las Vegas, 2011.
(55) Plancque, G.; Moulin, V.; Toulhoat, P.; Moulin, C. Europium Speciation by Time-Resolved Laser-Induced Fluorescence. *Anal. Chim. Acta* **2003**, *478*, 11−22.
(56) Runde, W. H.; Schulz, W. W. Americium. *Chemistry of the Actinide and Transactinide Elements* **2010**, 1339.
(57) Zhang, S.; Winter, P.; Wu, K.; Sherry, A. D. A Novel Europium(III)-Based MRI Contrast Agent. *J. Am. Chem. Soc.* **2001**, *123*, 1517−1518.
(58) Ganapathy, S.; Chacko, V.; Bryant, R.; Etter, M. Carbon CP-MASS NMR and X-Ray Crystal Structure of Paramagnetic Lanthanide Acetates. *J. Am. Chem. Soc.* **1986**, *108*, 3159−3165.
(59) Zhang, Y.-L.; Liu, W.-S.; Dou, W.; Qin, W.-W. Synthesis and Infrared and Fluorescence Spectra of New Europium and Terbium Polynuclear Complexes with an Amide-Based 1,10-Phenanthroline Derivative. *Spectrochim. Acta, Part A* **2004**, *60*, 1707−1711.
(60) Ohishi, T. Preparation and Properties of SiO2 Thin Films by the Sol-Gel Method Using Photoirradiation and Its Application to Surface Coating for Display. *Chemical Processing of Ceramics* **2005**, *20053072*, 425−428.
(61) Mason, H. E.; Harley, S. J.; Maxwell, R. S.; Carroll, S. A. Probing the Surface Structure of Divalent Transition Metals Using Surface Specific Solid-State NMR Spectroscopy. *Environ. Sci. Technol.* **2012**, *46*, 2806−2812.
(62) Rohm and Haas *AMBERCHROM™Chromatographic Resins*; 2005.

DOI: 10.1021/acsami.5b04481
ACS Appl. Mater. Interfaces 2015, 7, 20591−20599